ELEMENTA
Science of the Anthropocene

Mielke-Maday, I, et al. 2019. Methane source attribution in a U.S. dry gas basin using spatial patterns of ground and airborne ethane and methane measurements. *Elem Sci Anth*, 7: 13. DOI: https://doi.org/10.1525/elementa.351

RESEARCH ARTICLE

# Methane source attribution in a U.S. dry gas basin using spatial patterns of ground and airborne ethane and methane measurements

Ingrid Mielke-Maday[*,†], Stefan Schwietzke[*,†], Tara I. Yacovitch[‡], Benjamin Miller[*,†], Steve Conley[§], Jonathan Kofler[*,†], Philip Handley[*,†], Eryka Thorley[*], Scott C. Herndon[‡], Bradley Hall[†], Ed Dlugokencky[†], Patricia Lang[†], Sonja Wolter[*,†], Eric Moglia[*,†], Molly Crotwell[*,†], Andrew Crotwell[*,†], Michael Rhodes[*,†], Duane Kitzis[*,†], Timothy Vaughn[‖], Clay Bell[‖], Dan Zimmerle[‖], Russ Schnell[†] and Gabrielle Pétron[*,†]

An intensive coordinated airborne and ground-based measurement study was conducted in the Fayetteville Shale in northwestern Arkansas during September and October 2015 to compare and explain potential discrepancies between top-down and bottom-up estimates of regional natural gas (NG) methane ($CH_4$) emissions. In situ mobile downwind measurements are used to document the ethane to methane enhancement ratios (ERs) in emission plumes from NG operations in the region. Enhancement ratios are low (<2% for 87% of NG sources sampled) in this dry gas-producing region and normally distributed around 1.3% in the western half of the study area. A few sampled landfills emitted $CH_4$ but no ethane ($C_2H_6$). Sampling drives around large chicken farms, prevalent in the region, did not detect significant downwind $CH_4$ enhancements. In situ airborne measurements of $C_2H_6$ and $CH_4$ from area-scale surveys over and downwind of the region documented the resulting ERs from a mix of $CH_4$ sources. Based on these measurements, we show that on average during the measurement windows 85–95% of total $CH_4$ emissions in the western half of the Fayetteville Shale originated from NG sources, which agrees well with bottom-up estimates from the same field study. Lower mixing ratios measured over the eastern half of the region did not support the ER analysis due to the low signal-to-noise on $C_2H_6$ measurements.

**Keywords:** Methane; Emissions; Natural gas; Attribution; Fayetteville

## 1. Introduction

Methane ($CH_4$) is the primary component of natural gas (NG). Despite $CH_4$ being a potent greenhouse gas, when used as an alternative for power generation, NG can have a smaller climate impact than coal and oil, which each emit about twice as much carbon dioxide as NG per unit of energy delivered (EIA, 2016). However, losses to the atmosphere, which are estimated to be 2.3% of gross U.S. natural gas production (Alvarez et al., 2018) along the NG supply chain, can reduce its advantages. Natural gas systems were estimated to account for 25% of total U.S. anthropogenic $CH_4$ emissions in 2015 (EPA, 2017), making them the second largest national anthropogenic $CH_4$ source, behind enteric fermentation and above landfills (EPA, 2017). Within the NG sector, the largest fraction of $CH_4$ emissions, 66%, originates during the production phase (EPA, 2017).

Studies comparing top-down (atmospheric measurement based) and bottom-up (inventory/activity based) estimates of regional or national $CH_4$ emissions from oil and natural gas (O&NG) operations in the U.S. have pointed to systematic discrepancies between the two methods (Brandt et al., 2014; Zavala-Araiza et al., 2015). Aircraft campaigns in several U.S. O&NG basins have derived larger emissions of $CH_4$ and ethane ($C_2H_6$), another major component of NG, than estimated using available inventory data (Karion et al., 2013; Karion et al., 2015; Kort et al., 2016; Pétron et al., 2012; Pétron et al., 2014).

A major challenge for comparing regional top-down studies with O&NG emission inventories has been the quantitative attribution of top-down regional emission

* Cooperative Institute for Research in Environmental Sciences, University of Colorado Boulder, US
† NOAA Earth System Research Laboratory, US
‡ Aerodyne Research, Inc., US
§ Department of Land, Air, and Water Resources, University of California Davis, US
‖ Energy Institute and Department of Mechanical Engineering, Colorado State University, US
Corresponding author: Ingrid Mielke-Maday (Ingrid.mielkemaday@colorado.edu)

estimates between different sources of $CH_4$. The mass balance method used with aircraft data provides total $CH_4$ emissions for an area, which then must be apportioned between O&NG and other sources. To do so, previous top-down regional and national studies have often relied completely or partly on bottom-up information for $CH_4$ emissions apportionment or non-O&NG emissions estimation (Caulton et al., 2014; Karion et al., 2013; Pétron et al., 2012), even in cases where $C_2H_6$ was used to distinguish between sources (Peischl et al., 2015, 2016).

Atmospheric measurements of $CH_4$ alone, unless directly downwind of a point source (Conley et al., 2017; Frankenberg et al., 2016), are usually not enough to distinguish and separate contributions from different $CH_4$ sources. A few apportionment studies in O&NG fields have used alkane ratios or $CH_4$ isotopic signatures to distinguish between emissions from various $CH_4$ sources (Hopkins et al., 2016; Smith et al., 2015, 2017; Townsend-Small et al., 2015). However, results from these studies can be limited by a relatively small number of discrete samples or days of measurements. Additionally, mass balance and attribution methods using alkane or isotope enhancement ratios require subtracting local background values, which have not always been sufficiently documented (Schwietzke et al., 2017).

The work presented here is part of a larger coordinated intensive study conducted in the Fayetteville Shale dry gas play in north-central Arkansas in September and October 2015 to compare state of the science bottom-up and top-down regional NG $CH_4$ emission estimates. Emissions quantification at the facility or equipment level is presented by Bell et al. (2017), Conley et al. (2017), Robertson et al. (2017), Vaughn et al. (2017), Yacovitch et al. (2017), and Zimmerle et al. (2017). An aircraft mass balance estimate of spatially resolved $CH_4$ emissions from the study area on two consecutive days is described in Schwietzke et al. (2017), and a reconciliation between this top-down estimate and a bottom-up $CH_4$ emissions estimates is provided by Vaughn et al. (2018). The bottom-up model presented by Vaughn et al. revealed a strong diurnal variability in total NG $CH_4$ emissions, with the peak occurring during the mid-afternoon due to manual liquid unloading events at 107 wells over the two days modeled (Vaughn et al., 2018). Modeled bottom-up emissions estimates captured the same spatial variability in $CH_4$ emissions throughout the study area with a reasonable agreement in emissions estimates between the two approaches for the total study area, eastern half, and western half. NG $CH_4$ emissions normalized by natural gas production were found to be two times higher in the western half than in the eastern half (Schwietzke et al., 2017).

Presented here are atmospheric in situ $CH_4$ and $C_2H_6$ measurements from the ground and aircraft to apportion $CH_4$ emissions between NG operations and other sources in the Fayetteville dry shale gas field. $C_2H_6$ to $CH_4$ enhancement ratios in observed emission plumes (ERs, the molar ratio of $C_2H_6$ and $CH_4$ relative to their respective local background values) are compiled downwind of NG facilities in the Fayetteville Shale to characterize the spatial variability of NG ERs throughout the study area. These source ERs are then used together with total emission ERs from aircraft measurements to attribute $CH_4$ emissions between NG and other sources.

High frequency in situ measurements permitted the determination of enhancement ratios at more locations than would have been possible with discrete flask samples. The ability to quickly make measurements at a given location eliminated the need to correct for the species background, which can vary over time and space. The use of data collected on multiple days allows an assessment of the variability in ERs at different NG facilities and variability among ERs on flights across different days. This method is atmospheric measurement-based with incorporation of publicly available data and does not require inventory or operator-provided data. The unique combination of ground and aircraft data incorporates information about both source signatures and the mix of sources in the area into the attribution. Our work is an effort to further refine top-down measurement and attribution methods to help improve independent constraints on regional long-lived greenhouse gas emission attribution.

## 2. Methods

### *2.1. Overview*

The study area (**Figure 1**) comprised the core of the Fayetteville Shale production basin in Arkansas, USA, and spanned Cleburne, Conway, Faulkner, Independence, Jackson, Van Buren, and White counties to form an area ~65 km (north to south) by ~150 km (west to east). This area is a dry NG production region (Arkansas Geological Survey, 2015) with no oil production or processing of NG (Vaughn et al., 2018), and accounted for ~3.1% of national dry NG production in September 2015 (EIA, 2017). NG facilities in the area in 2015 totaled ~5500 active NG wells, 125 gathering stations, and six transmission stations. Variability in the $C_2H_6$ to $CH_4$ emission ratio for NG sources is expected to be due to variability in raw gas composition, as there is no gas processing at production facilities or at centralized locations. In addition to NG operations, potential $CH_4$ sources included agriculture (cattle and poultry farms), wetlands, geologic seeps, stationary combustion, and one small landfill in Faulkner County (Schwietzke et al., 2017). In the absence of biomass burning, only NG related sources in the study area are expected to co-emit $C_2H_6$ with $CH_4$. A fire ban was in effect in much of the study area during the study, so biomass burning is not expected to have occurred in the majority of the study area.

Fast response in situ $CH_4$ and $C_2H_6$ measurements were obtained using both ground-based and airborne platforms. An instrumented van (NOAA Global Monitoring Division (GMD) mobile laboratory) measured $CH_4$ and $C_2H_6$ in $CH_4$ emission plumes from public roads downwind of NG facilities in order to gather data needed to calculate representative ERs. $C_2H_6$ and $CH_4$ data were also collected by two mobile laboratories operated by Aerodyne Research, Inc. performing dual tracer flux ratio measurements, a downwind method used to determine facility-level $CH_4$ emissions (Roscioli et al., 2015; Yacovitch et al., 2017). A single-engine instrumented aircraft operated by Scientific Aviation was used to obtain the $C_2H_6$ and $CH_4$ data (Schwietzke et al., 2017) for regional-scale ERs that reflected the mix of $CH_4$ emissions in the study area.

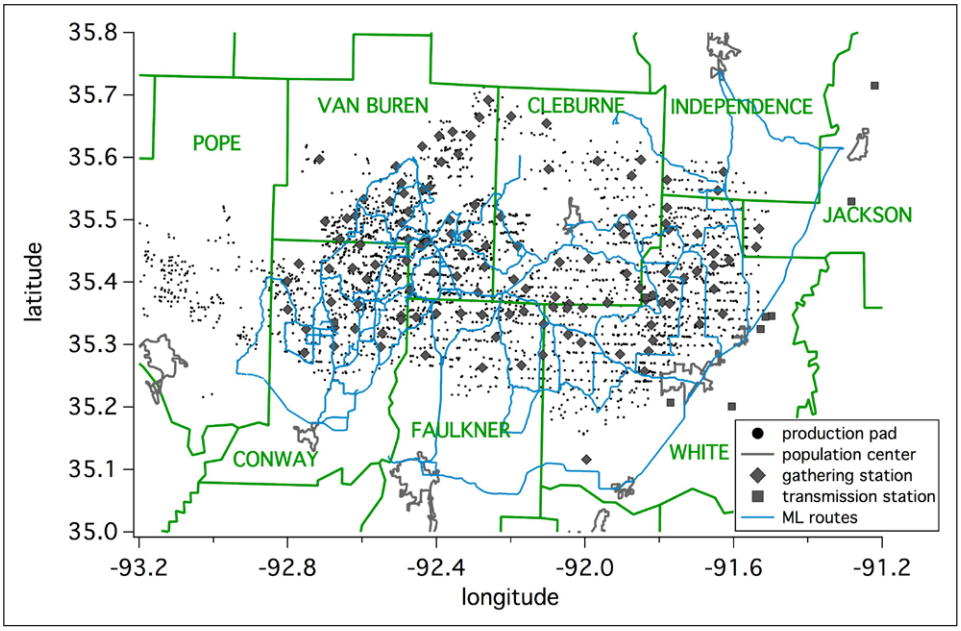


**Figure 1: Study area map.** Map of the study area marked with routes of NOAA ML drives with continuous measurements from September 23, 2015 through October 8, 2015. County outlines are shown in green. DOI: https://doi.org/10.1525/elementa.351.f1

Each platform's instrumentation and sampling strategy are described below.

### *2.2. Mobile laboratory and aircraft instrumentation and sampling strategy*

#### NOAA mobile laboratory

The NOAA mobile laboratory (ML), a 2005 Chevrolet 15 passenger van, was equipped with a four species cavity ring down spectrometer (CRDS) (Picarro model #G2401-m) that provided sequential measurements of $CH_4$, $CO_2$, and CO mole fractions, and measurements of water vapor every three seconds. A tunable infrared laser direct absorption spectroscopy (TILDAS) analyzer (Aerodyne Research, Inc.) with a 2990 $cm^{-1}$ laser measured $C_2H_6$, $CH_4$, and water vapor at 1 Hz. Stationary 1-sigma noise over 30 seconds under the deployment conditions was approximately 0.30 ppb on $CH_4$ for the CRDS, 0.05 ppb on $C_2H_6$, and 0.40 ppb on $CH_4$ for the TILDAS. Prior to and following ML drives each day, three gas standards prepared by NOAA GMD in Boulder, Colorado were measured by the CRDS and TILDAS instruments to identify potential instrument drift (see Supplemental Material). The ML was also equipped with a global positioning system (GPS) and NOAA GMD flask air sampling system. Further details of the ML set-up can be found in the Supplemental Material.

Discrete air samples, used to compare with in situ measurements, were collected using a programmable compressor package (PCP) and programmable flask packages (PFPs). The PCP contains the pump, batteries, and a microprocessor to control sampling, and the PFP consists of a manifold and twelve cylindrical, 0.7 L borosilicate glass flasks that are filled one by one (Aircraft Program Methods, 2018). These discrete air samples were analyzed by NOAA GMD using the same systems used for measurements in the Global Greenhouse Gas Reference Network (ESRL, 2017). $CH_4$ was analyzed by gas chromatography with flame ionization detection (Dlugokencky et al., 1994), and $C_2H_6$, by gas chromatography mass spectrometry (see Supplemental Material). $C_2H_6$ and $CH_4$ dry air mole fractions have 1-sigma uncertainties of 11 ppt (NOAA 2016 scale) and 1.1 ppb (NOAA X2004A scale), respectively.

#### Aerodyne mobile laboratory

Aerodyne Research, Inc. operated two mobile laboratories during the time when the NOAA ML was also deployed. Each housed TILDAS analyzers used for measuring $CH_4$, $C_2H_6$ and the trace gases used in their tracer release method for facility-level quantification of $CH_4$ emissions. Details of the mobile laboratory set-ups can be found in the supplemental material of Yacovitch et al. (2017).

#### Scientific aviation aircraft

Instrumentation onboard the Mooney Ovation aircraft included a NOAA GMD flask air sampling system, a cavity ring down spectrometer (Picarro model # 2301-f) with 0.5 Hz water-corrected measurements of $CH_4$ (<2 ppb uncertainty (Karion et al., 2013) $CO_2$, and water vapor, and a TILDAS $C_2H_6$ mini trace gas monitor (Aerodyne Research, Inc.). This instrument, with a 2997 $cm^{-1}$ laser, (~200 ppt noise in the configuration used in this study) was used to obtain 1 Hz measurements of $C_2H_6$. Though $C_2H_6$ values were not water-corrected (not removing water during calculations ignores dilution and results in a lower mole fraction than the dry air mole fraction), the highest water content observed on any flight (<2%) would necessitate a data correction that is small relative to the $C_2H_6$ signal observed on flights. Additional instrumentation included a Vaisala relative humidity and temperature probe and GPS (Hemisphere VS101). Details of the aircraft set-up can be found in Conley et al. (2017).

### *2.3. Methane emission source attribution model*

A top-down attribution of $CH_4$ emissions between NG and other $CH_4$ sources was accomplished using the approach

described below. Atmospheric ER measurements are assumed to be equivalent to emission ratios from $CH_4$ sources since the average global atmospheric lifetimes of $C_2H_6$ and $CH_4$ (approximately 2 months and 9 years, respectively (Rudolph and Enhalt, 1981; Nisbet et al., 2016)) make chemical losses negligible when examining plumes and air masses downwind of a facility or source region over timescales on the order of minutes to a few hours. It is assumed that the ER from a given source in the study area does not change from hour-to-hour or day-to-day due to the fact that the produced gas is dry and there are no gas treatment facilities or liquid condensate collection activities in this basin. Results presented in a later section support this assumption.

For an area of interest, the total $CH_4$ and $C_2H_6$ emissions (E) can be separated into the contributions from NG and other sources (denoted "other").

$$E(CH_4)_{total} = E(CH_4)_{NG} + E(CH_4)_{other} \quad \text{Eq. 1}$$

$$E(C_2H_6)_{total} = E(C_2H_6)_{NG} + E(C_2H_6)_{other} \quad \text{Eq. 2}$$

$C_2H_6$ emissions from other sources, such as biomass and biofuel burning, are assumed to be negligible within the study area. There was a fire ban in effect for a large part of the study area at the time of the study. Therefore,

$$E(C_2H_6)_{other} \approx 0 \quad \text{Eq. 3}$$

$$E(C_2H_6)_{total} = E(C_2H_6)_{NG} \quad \text{Eq. 4}$$

Equations 1 and 2 are rewritten below to use area mean quantities constrained with field measurements. The NG facility plume ERs determined from ML data are used to constrain an area mean $ER[C_2H_6/CH_4]_{NG}$ in Eq. 6. The area-scale plume ERs from aircraft data, which represent the mix of $CH_4$ sources in the study area, are used to constrain an area mean $ER[C_2H_6/CH_4]_{area}$ in Eq. 5.

$$E(CH_4)_{total} = E(C_2H_6)_{total} * \frac{1}{ER\left[\frac{C_2H_6}{CH_4}\right]_{area}} = E(C_2H_6)_{NG} * \frac{1}{ER\left[\frac{C_2H_6}{CH_4}\right]_{area}} \quad \text{Eq. 5}$$

$$E(CH_4)_{NG} = E(C_2H_6)_{NG} * \frac{1}{ER\left[\frac{C_2H_6}{CH_4}\right]_{NG}} \quad \text{Eq. 6}$$

The relative contribution of $CH_4$ from NG related sources in the study area can thus be calculated using Eq. 7, the ratio of Eq. 6 to Eq. 5.

$$\frac{E(CH_4)_{NG}}{E(CH_4)_{total}} = \frac{ER\left[\frac{C_2H_6}{CH_4}\right]_{area}}{ER\left[\frac{C_2H_6}{CH_4}\right]_{NG}} \quad \text{Eq. 7}$$

The result is a mean estimate of the fraction of the total $CH_4$ emissions that originate from NG sources in the area of interest during the time of the campaign.

This model is only applicable in cases in which there are only two distinct $CH_4$ source categories with a small range of ERs, as another $CH_4$ source with its own characteristic ER would introduce another mode in the ER distribution and would require another independent trace gas marker and more equations to constrain the attribution. As previously stated, all $C_2H_6$ enhancements are assumed to originate from NG related sources, and the ER distribution for NG point source emissions and regional area source plumes is assumed constant over the time period of the study.

### 2.4. Mobile laboratories and aircraft sampling strategies

#### NOAA mobile laboratory

Twelve daytime drives were conducted with the NOAA ML, ranging from six to ten hours each (typically from about 10:00–18:00 local time), to compile ERs in $CH_4$ plumes throughout the study area. Drives were made on public roads throughout extensive portions of the study area, as shown in **Figure 1**. Distances from the ML on the road to a facility were typically 0.05 to 0.30 km.

When a $CH_4$ emission plume (at least 50 ppb above local background) was observed downwind of a potential emission source, the ML was intentionally positioned to acquire 30 seconds to a few minutes of in situ data to measure multiple $CH_4$ plumes to calculate the ER, check for temporal stability in the ER at the source, and in some instances, collect flask air samples in the local background air and in the facility emission plume. When collecting in situ data, the ML was driven slowly out of the $CH_4$ plume to allow $CH_4$ to return to its background level. In this way, a range of $CH_4$ and $C_2H_6$ mole fractions could be measured and a slope calculated to determine an ER. Section 3.1 provides an assessment of the temporal consistency of ERs when measurements at the same facility were repeated on multiple days.

To collect flask air samples, the ML engine was first turned off. Then, the PFP sampling manifold and flask were first flushed (at ~10 and ~17 SLPM, respectively) for 45 seconds and, when complete, air sample collection was manually triggered using the real-time display of in situ measurements to target different mole fractions. Fill times were ~10 seconds. The core GMD chemical analysis instrumentation focuses on tracking background air composition, and to avoid contamination of the GC-FID columns used to measure samples in the Global Greenhouse Gas Reference Network, we intentionally only collected PFP air samples with $CH_4$ mole fractions below 5 ppm.

#### Aerodyne mobile laboratory

Included in our analysis are ERs from Aerodyne Research, Inc. for which: (i) the $CH_4$ emissions at the NG facility could be determined using the dual tracer release method, (ii) there was a coefficient of determination of 0.50 or greater, and (iii) manual inspection of the $CH_4$ and $C_2H_6$ plumes did not indicate any problems with the Aerodyne dual tracer release at the target site, as described in Section 6

of the Supplemental Material in Yacovitch et al. (2017). Here we use only ERs for which the reported 95% confidence interval is less than or equal to 30% of the mean ER, leaving 46 of the original 49 facilities at which ERs were obtained by Yacovitch et al. (2017).

#### Scientific aviation aircraft

Fifteen flights were conducted between September 21 and October 14, 2015. Data from October 1 and October 2 were used by Schwietzke et al. (2017) to calculate a total $CH_4$ emission estimate for the study area using a mass balance approach. Flights with box, raster, or spiral sampling patterns were conducted over the entirety and subsections of the study area to gather data for $CH_4$ emission quantification, $CH_4$ source attribution, and individual facility $CH_4$ emission quantification, respectively (see Supplemental Material). Aircraft measurements from five raster flights, the paths of which are shown in **Figure 2**, were used to investigate mean ERs for the western and eastern halves of the study area.

### *2.5. Analysis of ground measurements in facility-level plumes*

Mobile laboratory data were used to determine representative ERs for NG sources in the study area. $CH_4$ plumes measured by the ML were identified in $CH_4$ data from the CRDS using an instantaneous 50 ppb $CH_4$ enhancement threshold above the local $CH_4$ background. This threshold was chosen to distinguish enhancements caused by local emissions from instrument noise and background variability without biasing plume selection toward relatively large $CH_4$ plumes. The start time of each plume was determined by the time immediately before $CH_4$ increased by 50 ppb and the end time was determined by the time $CH_4$ returned to its start time $CH_4$ value, with low variability in $CH_4$ prior to and following the plume. Plumes were identified by manually screening the time series multiple times to prevent omissions and errors. If data were acquired when the ML was moving, only plumes less than one minute in duration were included in the analysis to avoid including multiple facility plumes and potentially varying background levels. Using code described by Yacovitch et al. (2014), a $C_2H_6$ vs. $CH_4$ scatterplot was created for each plume with data from the TILDAS, and the ER for each plume was determined using the slope calculated by orthogonal distance regression. Because the $C_2H_6$ and $CH_4$ data were acquired from the same absorption spectra on the same instrument, no sampling time offset optimization was required. Additionally, no assignment of $C_2H_6$ and $CH_4$ background was needed for each plume because in the method described above, the background is accounted for in the intercept of the scatterplot and the slope determined by enhancements alone, reflecting the $C_2H_6$ to $CH_4$ ratio in isolated plumes.

An ER was assigned to a source only if the coefficient of determination, $R^2$, was at least 0.65. For $CH_4$ sources where more than one ER was determined, a time-weighted

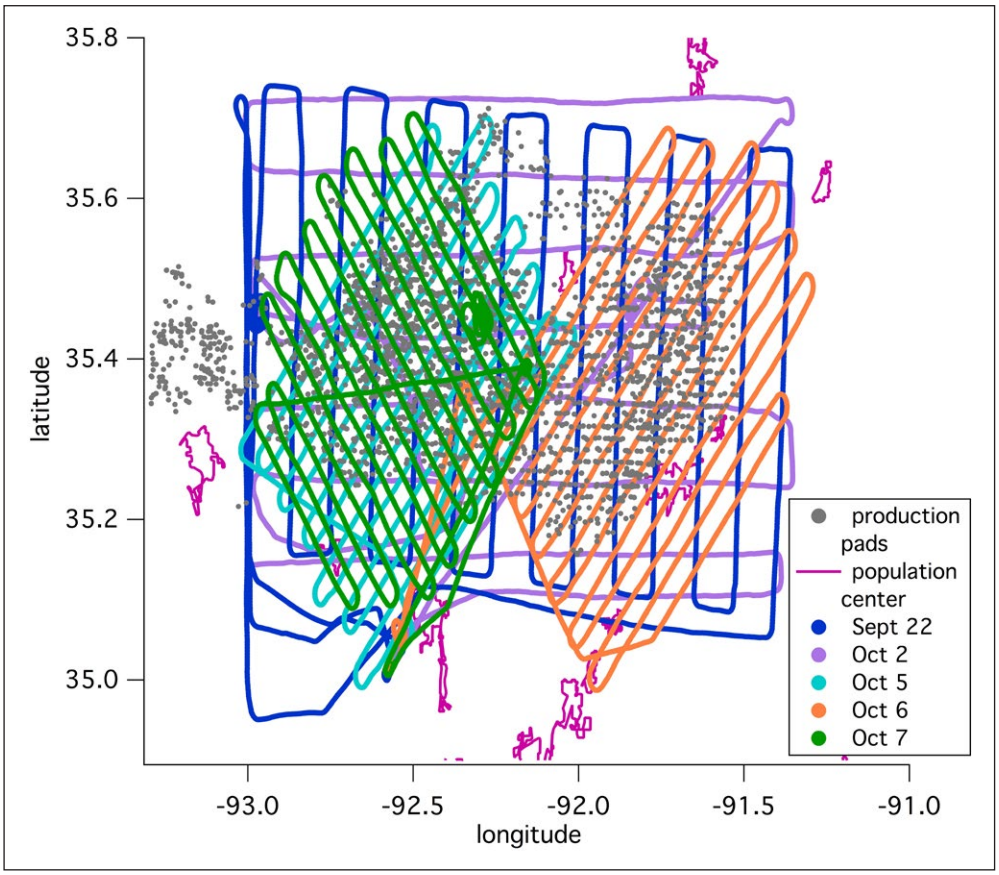


**Figure 2: Map of raster flights used for ER calculations.** Five raster flights, conducted on September 22, October 2, October 5, October 6, and October 7, 2015, were used to obtain area-scale ERs. DOI: https://doi.org/10.1525/elementa.351.f2

average was calculated to assign a single mean ER to the source. Only results for which a facility location could be readily identified as the emission plume source are presented. $CH_4$ plumes that could not be attributed to a specific source are not included in the analysis. Plumes from 71 NG facilities measured by the NOAA ML passed the filtering criteria and though the minimum $R^2$ required was 0.65, 85% of the NG plumes had an $R^2$ associated with the ER that was 0.95 or greater.

### 2.6. Analysis of aircraft measurements for area-scale plumes

Aircraft measurements in the boundary layer over the study area were used to determine area-scale plume ERs (see Eq. 5). The portion of the data for which $CH_4$ was enhanced above background was identified on downwind transects (for box pattern flights) and legs (for raster pattern flights) and an ER was calculated using orthogonal distance regression weighted by the airborne instrumentation noise of 1.3 ppb for $CH_4$ (Karion et al., 2015) and 200 ppt for $C_2H_6$. We divide the study area into western and eastern halves using –92.1° longitude according to observed spatial differences in aircraft-based $CH_4$ emission estimates normalized by NG production (Schwietzke et al., 2017). In the event that multiple transects or legs from a single flight were downwind of the study area, the ERs for all transects or legs were averaged. Typical ranges observed while flying transects were approximately 1940 to 2300 ppb for $CH_4$ and 1.6 to 4.0 ppb for $C_2H_6$. Mole fractions observed in the aircraft data are lower than those observed in the ML, where $CH_4$ and $C_2H_6$ enhancements very close to sources could be up to several thousand ppb $CH_4$ and several hundred ppb $C_2H_6$. As the aircraft measured downwind of different regions of the study area, background $CH_4$ levels sometimes changed. To distinguish background variability from emission sources, ERs were determined only for those subsections of a leg or transect that included $CH_4$ enhancements of at least 50 ppb.

Criteria for acceptance of ERs were that measurements were made in the planetary boundary layer, a $CH_4$ enhancement in area plumes of at least 50 ppb above background and a $C_2H_6$ enhancement of at least 1 ppb to ensure a high enough signal to noise ratio, and a coefficient of determination of at least 0.65. After filtering using the above criteria, flight pattern, and wind direction, five flights could be used in the determination of an area ER for the western half of the study area. Several transects in these flight and others had low signal to noise and low enhancements, disqualifying them for use in ER calculations. Low signal to noise occurred due to low $CH_4$ and $C_2H_6$ enhancements in the planetary boundary layer and was observed more often over the eastern half of the study area, where total $CH_4$ emissions were found to be lower than in the western half (Schwietzke et al., 2017).

## 3. Results and Discussion

### 3.1. Mobile laboratory drives

#### Facility plume $C_2H_6$ to $CH_4$ enhancement ratios on different days

Seven of eight facilities at which plume measurements were repeated over multiple days show consistent (difference <20%) ERs across days, as shown in **Table 1**. This excludes 106 facilities with measurements on only one day (see next subsection). ERs shown in **Table 1** are for each plume measured at the facility rather than the time-weighted average for the facility. All ERs have an $R^2$ of 0.65 or greater, and 85% of the NG plumes had an $R^2$ associated with the ER that was 0.95 or greater. The repeatability of

**Table 1: NOAA ML repeat ER measurements.** All in situ $C_2H_6$ to $CH_4$ ERs measured by the ML at the same facilities over multiple days. DOI: https://doi.org/10.1525/elementa.351.t1

| Facility type | Date | In situ $C_2H_6$ to $CH_4$ ER |
|---|---|---|
| Production pad 1 | 9/29/2015 | 1.3% |
| | 10/3/2015 | 1.3% |
| Production pad 2 | 9/24/2015 | 0.9% |
| | 10/2/2015 | 0.9% |
| Production pad 3 | 9/25/2015 | 1.6% |
| | 9/30/2015 | 1.6% |
| | 10/5/2015 | 1.9% |
| Production pad 4 | 9/24/2015 | 1.3% |
| | 10/2/2015 | 1.3% |
| Production pad 5 | 9/30/2015 | 0.9% |
| | 10/5/2015 | 1.1%, 1.1% |
| Production pad 6 | 10/1/2015 | 1.5% |
| | 10/5/2015 | 1.5% |
| Production pad 7 | 9/24/2015 | 0.8%, 0.9%, 0.9%, 0.9%, 1.0%, 5.3%, 5.9%, 11.6% |
| | 9/28/2015 | 0.9%, 0.9%, 0.9%, 0.9%, 0.9%, 1.0% |
| | 10/2/2015 | 0.9% |
| Gathering station | 9/29/2015 | 1.4%, 1.4% |
| | 10/3/2015 | 1.4%, 1.4%, 1.4% |

ERs on different days at these facilities suggests that an ER measured at a facility by the ML on any given day can be used as a representative value for that facility even without repeated measurements on different days and that emission ratios at NG facilities were likely constant over the course of the study. The spread in ERs observed at Production Pad 7 on September 24 suggests another emission source in addition to vented gas. $CH_4$ plumes at this pad that are enhanced in $C_2H_6$ also show a strong correlation with the combustion product, $CO_2$ (see Supplemental Material), though no correlation between CO and $CH_4$ was observed. The most likely sources of combustion at production pads in this dry gas basin are on-site NG-powered compressor engines, used at some production pads to increase flow from a well. It is possible that the natural gas-fueled compressor was running at the time of the ML measurements, though the activity data needed for confirmation are not available. Using ERs only from plumes for which the $CH_4$ enhancement was at least 50 ppb, the time-averaged ER for production pad 7 is 1.7%.

Low temporal variability between ERs at a NG facility is expected because the ER from mostly fugitive (in this region) emissions is dependent upon the composition of the raw natural gas being extracted, which remains constant over the timescale at which this study was conducted. However, variability in natural gas composition due to geologic differences throughout a region can lead to spatial variability in ERs.

### Range and spatial distribution of $C_2H_6$ to $CH_4$ ERs observed at different NG facility types

In this section, we present ER results from the 114 NG facilities measured by the NOAA ML and the Aerodyne mobile laboratories (AML) (Yacovitch et al., 2017). For the three facilities that were measured by both NOAA and the AML, the ERs at both gathering stations are identical (1.0% and 1.4% for the two gathering stations) and within 10% for the production pad (1.1% measured by NOAA and 1.0% measured by the AML). The dataset presented from this point forward consists of results from both mobile laboratories.

ERs in NG facility plumes, including production pads, gathering stations, transmission stations, pipelines and dehydrator stations, display some spatial variability throughout the study area, especially on the eastern side, as shown in **Figure 3**. **Table 2** shows the range of ERs observed at each type of NG facility measured on the ground in the western and eastern halves of the study area. The sample size of three of the NG source types (pipeline junctions, dehydrator stations, and transmission stations) is small, making it

**Table 2: ER ranges by facility type.** Range of ERs in plumes sampled downwind of NG facilities in the western and eastern halves of the study area by the NOAA and Aerodyne MLs. DOI: https://doi.org/10.1525/elementa.351.t2

| Source type | West ER | Sample size | East ER | Sample size |
|---|---|---|---|---|
| Production pads | 0.8–2.1% | 52 | 0.9–7.8% | 20 |
| Gathering stations | 1.0–1.7% | 26 | 1.1–7.9% | 10 |
| Pipeline junction | N/A | 0 | 3.9% | 1 |
| Dehydrator station | N/A | 0 | 4.0% | 1 |
| Transmission station | 2.0% | 1 | 1.6–5.7% | 3 |

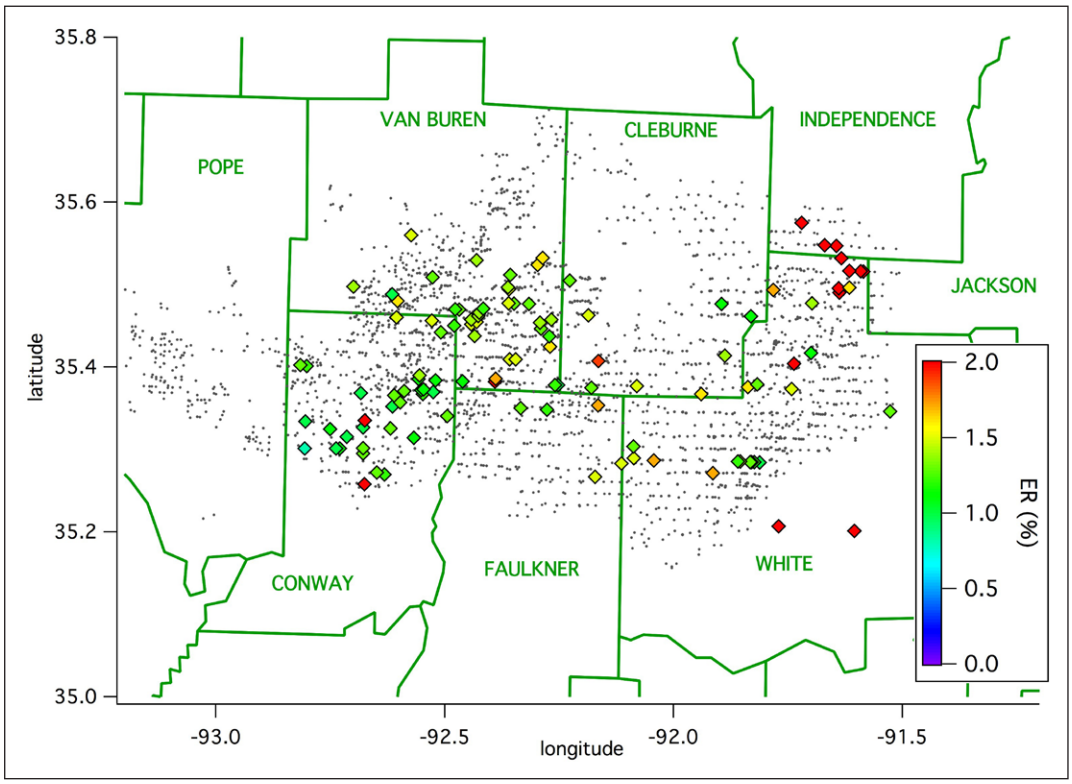


**Figure 3: Spatial variability of ERs in the study area.** Mean facility-level NG ERs determined from ML measurements. DOI: https://doi.org/10.1525/elementa.351.f3

difficult to draw conclusions about the observed ER ranges at these types of facilities. More measurements were made throughout the study area at production pads and gathering stations, which represent the majority (~98%) of the active facilities and about 97% of estimated $CH_4$ emissions (Vaughn et al., 2018) in the study area. Production pads and gathering stations display similar ER ranges of 0.8 to 7.8% and 1.0 to 7.9%, respectively. The similar ER ranges between these two types of facilities are to be expected given the lack of gas processing in this dry gas field, which has very low water and non-methane hydrocarbon content and no co-produced natural gas condensate or oil.

The ranges of ERs observed at production pads are similar to gathering stations within the western half and within the eastern half of the study area. In the western half, production pad ERs range from 0.8 to 2.1% and gathering stations from 1.0 to 1.7%. In the eastern half, production pad ERs range from 0.9 to 7.8% and gathering stations from 1.1 to 7.9%. Facilities in the eastern half have a greater range of ERs that tend toward higher values. Only one of 13 facilities with an ER of 2.1% or greater is located in the western half. Of the remaining facilities with relatively high ERs, all of which are located in the eastern half, eight are located in White county (2.1–5.7%), and four are located in Independence county (6.2–7.9%). Though the range of ERs observed at NG facilities in the eastern half is larger, facilities with relatively high ERs tend to be in the same geographic subregion of the study area (see **Figure 3**).

At the gathering station at which a 7.9% ER was observed, combustion was evident, as $CH_4$ plumes correlated with both $CO_2$ and CO. At gathering stations, which have on-site compressors, combustion processes are expected but $CH_4$ correlation with combustion tracers was observed at only one of the eight gathering stations surveyed by the NOAA ML. It is possible that at the other stations, hot combustion plumes rose too high and that the ML was not far enough downwind to be able to measure the plume where it reached the surface. However, even though combustion occurs at compressor stations, higher ERs at these facilities are not necessarily expected because combustion slip (unburned fuel in the compressor engine exhaust) has been shown to be the main source of $CH_4$ emissions at gathering stations in the study area (Vaughn et al., 2017).

**Figure 4** shows the distribution of ERs measured at NG facilities by the MLs. The majority (64%) of NG ERs observed in the western half range from 1.2 to 1.5%, with a mode of 1.3%. The eastern half has a similar range of frequent ERs of 1.2 to 1.5% with a peak in the distribution at 1.3% also. However, there is significant variability in ER in the eastern half, where 34% of measured facilities have ERs of 2% or greater. Higher ERs in the eastern half are confirmed by comparison with $C_2H_6$ to $CH_4$ ratios from gas composition data provided by operators for a subset of production pads and gathering stations (**Figure 5**). In cases where results from multiple gas composition samples were provided for a facility, the mean $C_2H_6$ to $CH_4$ ratio was used. Gas composition data exhibit modes for both the western and eastern halves of 1.3 to 1.5% respectively, consistent with ML plume data. Composition data also reveal a portion of facilities in the eastern half with $C_2H_6$ to $CH_4$ ratios greater than 2%. This portion is 28% compared with the 34% determined by ML measurements. Like the ML results, all facilities in the eastern half with $C_2H_6$ to $CH_4$ ratios of at least 2% are located in White and Independence counties. Higher ERs in the eastern half are likely a result of the thermal maturity of the geologic formation being drilled. Thermal maturity refers to the extent to which reactions involving heat that convert organic matter to oil and natural gas have occurred. Generally, natural gas is expected to be wetter (higher $C_2H_6$ to $CH_4$ ratio) as the thermal maturity of its source rock decreases (Visschedijk et al., 2018).

In the Barnett Shale play in Texas, where natural gas is produced throughout the entirety of the study area, the distribution of 172 NG ERs measured by Yacovitch et al. (2015) showed a peak at approximately 1.5%. The highest ERs were observed in the northwest, where oil is co-produced.

The aircraft performed spiral flight patterns around several potential $CH_4$ sources, including non-NG sources, and ERs were calculated. Although results are not used in the attribution, they can be found in the Supplemental Material.

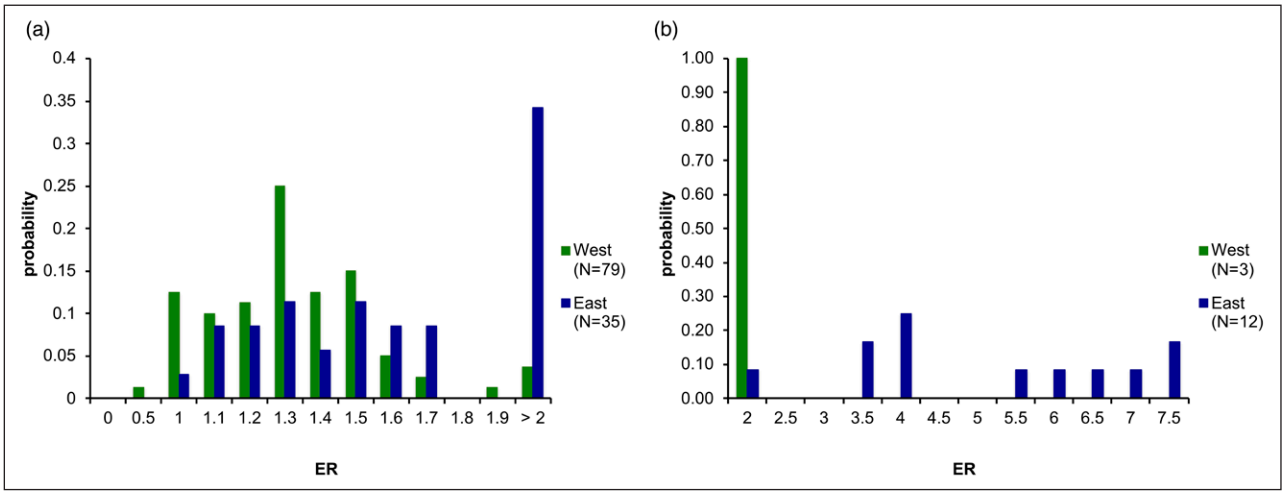


**Figure 4: ER distributions from ML measurements. (a)** Distribution of the 114 NG ERs compiled by the NOAA and Aerodyne MLs. **(b)** Same as (a) but for NG ERs ≥2%. DOI: https://doi.org/10.1525/elementa.351.f4

### Measurements at poultry farms

Arkansas is among the top states for the production of poultry in the United States, ranking third and fourth for broiler production in terms of head of chickens and pounds produced, respectively, in 2015 (USDA, 2015). While chickens are not known to be a $CH_4$ source as a result of enteric fermentation like cattle, $CH_4$ could be emitted from their manure (Monteny et al., 2001). Chicken litter, a combination of manure and the bedding in the chicken house, is often temporarily stored on-site until it can be removed and applied as a fertilizer for crops. However, best management practices recommend covered (dry) storage, which serves to minimize the potential for $CH_4$ and ammonia production (Ogejo et al., 2009).

Commercial poultry farms in the study area were long enclosed buildings with fans for ventilation and no visible liquid manure storage ponds. Measurements were made downwind of nine poultry farms (see Supplemental Material for locations), identified by the strong downwind localized smell of ammonia. At the time of the study, 292 poultry farms were known to be in the study area. Using the same 50 ppb threshold above the local background as was used to identify NG $CH_4$ plumes, poultry farms exhibited no substantial $CH_4$ enhancements. For a poultry farm measurement shown in **Figure 6**, $CH_4$ enhancements were approximately 10 ppb during each ML transect. For comparison, background variability for surface $CH_4$ on ML drives had a range of approximately 300 ppb. Based on these data, it is

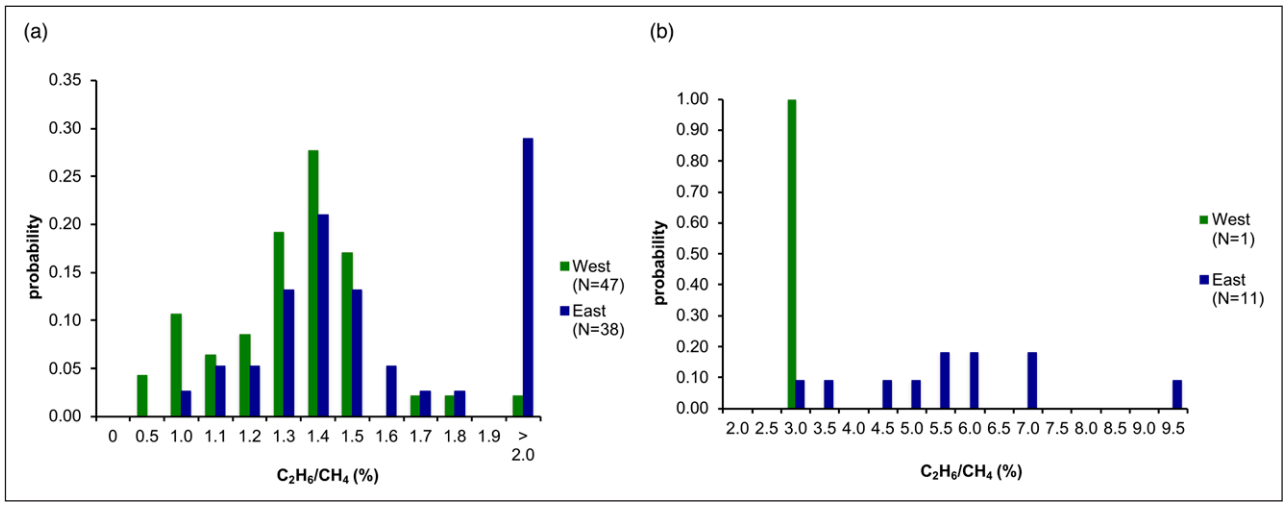


**Figure 5: Ratio distributions from operator gas composition data. (a)** Distribution of gas composition $C_2H_6$ to $CH_4$ ratios at production pads and gathering stations using 2015 gas composition data provided by local NG facility operators. **(b)** same as (a) but for ratios ≥2%. DOI: https://doi.org/10.1525/elementa.351.f5

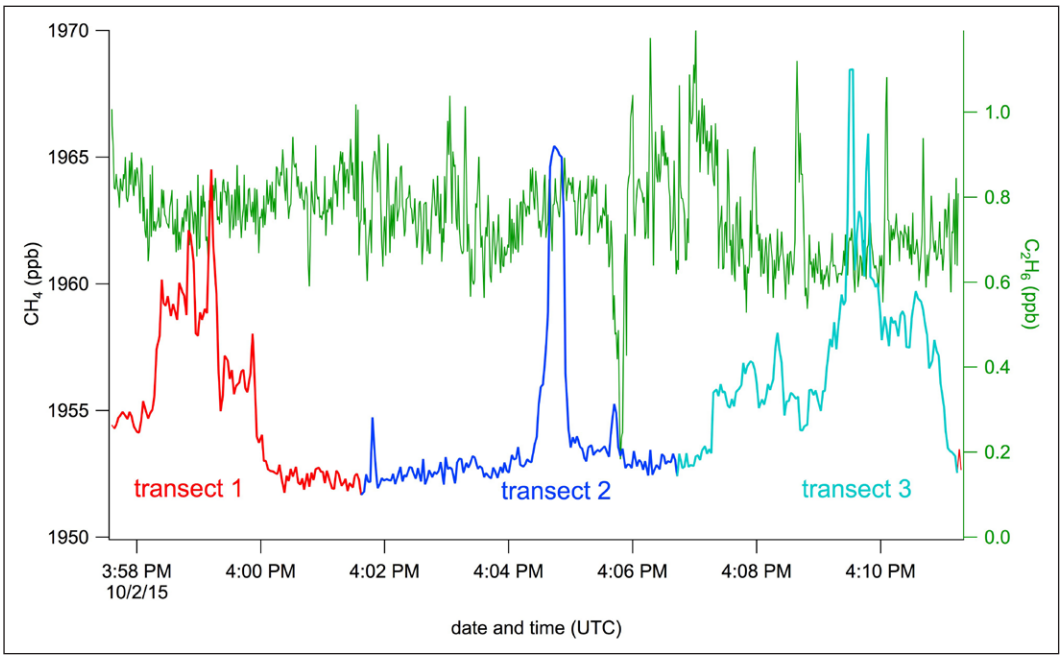


**Figure 6: Poultry farm ML downwind measurements.** Time series of measurements collected downwind of a poultry farm at which the ML performed three successive downwind transects. $CH_4$ (red, blue and turquoise) is from the CRDS and $C_2H_6$ (green) from the TILDAS. Peak $CH_4$ enhancements are on the order of 10 ppb, not a significant enhancement compared to the 50 ppb threshold used for this study and the levels detected downwind of NG facility plumes. DOI: https://doi.org/10.1525/elementa.351.f6

not expected that poultry contributed significantly to total $CH_4$ emissions in the study area. The bottom-up $CH_4$ emissions estimate for poultry farms provided by Schwietzke et al. (2017) of <200 kg $CH_4$/hr for the entire study area also suggests that poultry farms are a small source of $CH_4$ emissions when compared to the total (30.6 tons $CH_4$/hr).

#### Determination of mean NG $C_2H_6$ to $CH_4$ ERs

To derive mean ERs for the full study area as well as the western and eastern halves, we calculate spatially distinct means of the ML NG facility plume ERs weighted by NG production volumes using a Delaunay Triangulation (see Supplemental Material). This method accounts for spatial variability in the ER across each half and for sections of the study area with less measurement coverage than others. The Delaunay Triangulation algorithm in MATLAB connects the ER measurement locations into triangles (using their GPS coordinates) so that no other measurement location lies in a circumcircle of a given triangle and the value of the minimum angle of each triangle is maximized (See Figure S5). The varying sizes of the resulting triangles account for disparity in measurement density in the study area and ensure that there are no triangles without associated ER measurements. Each vertex of a triangle represents a measured ER. For each triangle, the three ERs are averaged and the mean value is assigned as the mean ER for all NG emissions in that triangle. Using September 2015 NG production data from the Arkansas Oil and Gas Commission (AOGC) (AOGC, 2015), the NG production of all production pads contained within each triangle was summed. With this production data and the mean ER for each triangle, a production weighted mean NG ER was calculated for the study area, western half, and eastern half.

A simulation was performed in which a simple random sample of 80% of the NOAA and AML facility ER data points was selected without replacement and the Delaunay Triangulation method was applied. Performing this simulation 30 times generated a mean ER and standard deviation, which was used to assign an uncertainty to the mean NG ERs generated by Delaunay Triangulation. The resulting mean NG ERs are 1.68 ± 0.10% for the full study area, 1.34 ± 0.03% for the western half, and 2.10 ± 0.22% for the eastern half.

### 3.2. Determination of area-scale $C_2H_6$ to $CH_4$ ERs from aircraft data

While ML data were used to determine ERs characteristic of NG operations in the study area, aircraft data were used to calculate area-scale ERs that include $CH_4$ emissions from all sources in the study area. $CH_4$ plumes measured by the aircraft are from a combination of multiple point sources after emissions have been transported from their sources and mixing has occurred downwind. NG source ERs and area-scale ERs were then combined (Eq. 7) to estimate the portion of the total $CH_4$ emissions in the study area originating from NG operations.

Area-scale ERs were calculated by fitting orthogonal distance regression slopes through the $C_2H_6$ vs. $CH_4$ in situ aircraft measurements for multiple flight legs in the boundary layer downwind of or over the study area and calculating a mean for each flight. The resulting aircraft ERs are shown in **Table 3**. ERs for each transect or leg of each flight used for attribution can be found in the Supplemental Material.

**Figure 7A** shows an example raster flight track for the determination of an ER for one leg (leg 4). For this flight on October 5, 2015 with wind from the North, $CH_4$ enhancements were observed over the western half of the study area, beginning with leg 4 (starting upwind in the northwestern corner and moving further southeast). The portion of leg 4 for which $CH_4$ is enhanced is shown with a box in **Figure 7B** and the corresponding $C_2H_6$ to $CH_4$ scatterplot in **Figure 7C**. The slope is 1.25 ± 0.04% ($R^2$ = 0.88).

Representative area-scale ERs were calculated for the western half using five raster flights conducted on September 22, October 2, October 5, October 6 and October 7, 2015 (**Table 3**), and a mean $C_2H_6$ to $CH_4$ slope for the enhancements observed over and/or downwind of the western half of 1.21 ± 0.02% was calculated.

While this result is higher than the 0.6% determined by Peischl et al. (2015) from two flights over the Fayetteville Shale, the ER reported in this study is only for the western half of the study area, whereas the 0.6% reported by Peischl et al. is for the entire region. The mean area-scale ER of 1.21 ± 0.02% from this study falls within the range of ~1–3% from dry gas sources with a mode of 1.8% determined from flights in the Barnett Shale (Smith et al., 2015).

Larger enhancements over the western half permitted calculation of area-scale ERs whereas in the eastern half, $C_2H_6$ signal with the same magnitude as the measurement noise made calculating ERs impossible. $CH_4$ emissions from NG operations normalized by NG production were found to be about one half in the eastern half relative to the western half on two days (Schwietzke et al., 2017). Since $C_2H_6$ is co-emitted with $CH_4$, it is likely that $C_2H_6$ emissions are also lower in the eastern half, and a

**Table 3: Area-scale ERs determined from aircraft measurements.** Area-scale ERs for the western half determined using aircraft data for each flight for which analysis was possible. DOI: https://doi.org/10.1525/elementa.351.t3

| Date | Time window of measurements (local time) | Altitude range (meters above ground level) | $CH_4$ range (ppb) | $C_2H_6$ range (ppb) | $R^2$ range and number of legs | Mean $C_2H_6$ to $CH_4$ ER (in situ) |
|---|---|---|---|---|---|---|
| 9/22/2015 | 3:56 PM–4:12 PM | 403–735 | 1910–2050 | 1.3–3.7 | $R^2$ = 0.69 for 1 leg | 1.2 ± 0.03% |
| 10/2/2015 | 12:47 PM–1:13 PM | 244–460 | 1940–2080 | 1.2–2.9 | $R^2$ = 0.64 for 1 leg | 1.1 ± 0.04% |
| 10/5/2015 | 12:09 PM–2:05 PM | 157–444 | 1999–2337 | 2.3–8.4 | $R^2$ from 0.67 to 0.91 for 7 legs | 1.2 ± 0.03% |
| 10/6/2015 | 11:04 AM–12:09 PM | 198–466 | 1990–2236 | 2.3–5.7 | $R^2$ from 0.65 to 0.91 for 4 legs | 1.3 ± 0.05% |
| 10/7/2015 | 12:41 PM–3:19 PM | 138–560 | 1939–3500 | 1.2–11.4 | $R^2$ from 0.67 to 0.90 for 10 legs | 1.3 ± 0.04% |

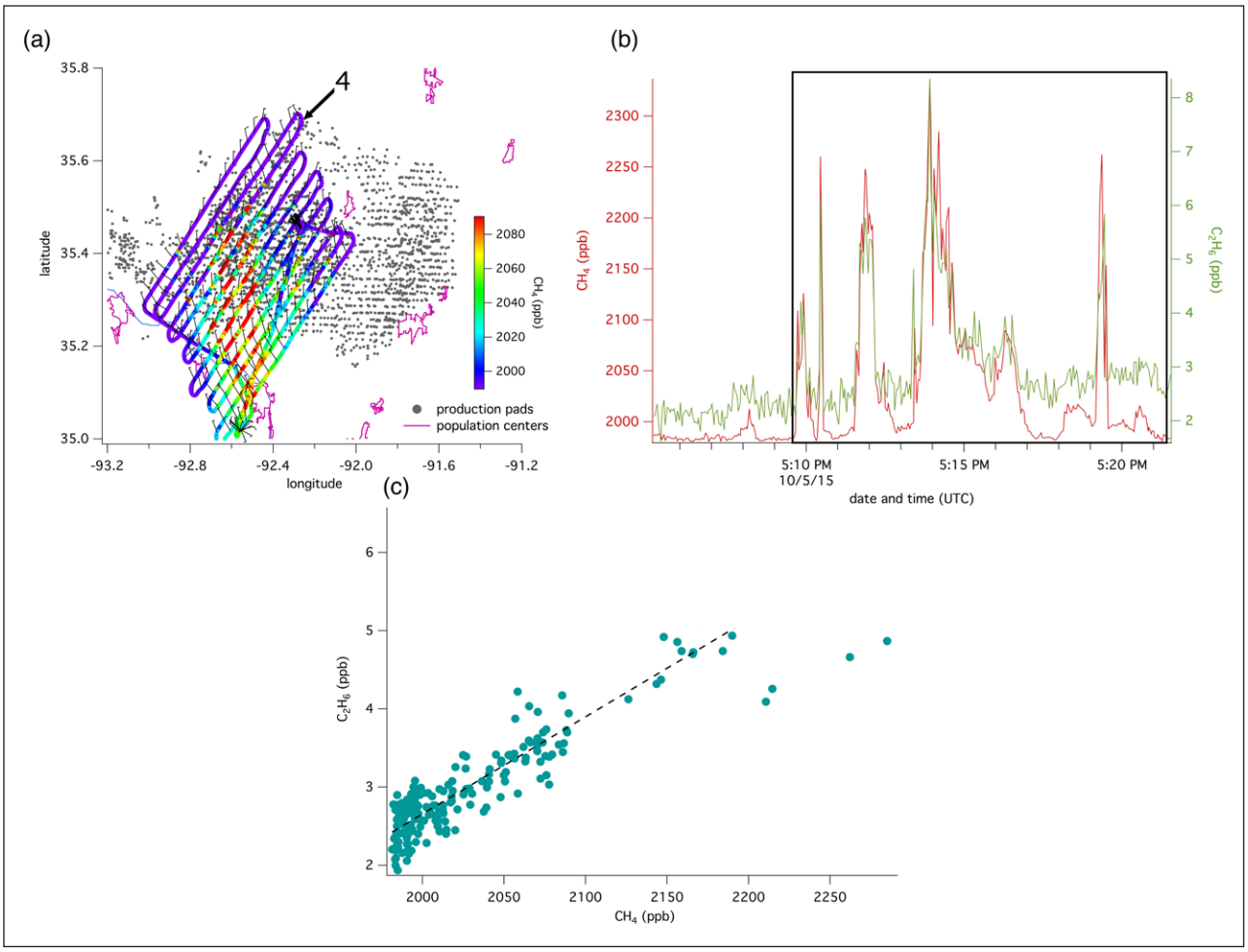


**Figure 7: Example of ER determination process for an aircraft leg. (a)** October 5, 2015 flight track color-coded by $CH_4$. Leg 4 is labeled. **(b)** The $C_2H_6$ and $CH_4$ time series for leg 4. The box indicates the region where $CH_4$ is enhanced over background. **(c)** The $C_2H_6$ vs. $CH_4$ scatterplot of the data from the $CH_4$ enhanced portion of leg 4 fit with an orthogonal distance regression line. DOI: https://doi.org/10.1525/elementa.351.f7

spatially-resolved bottom-up $CH_4$ emissions inventory of the total study area showed no substantial differences in non-NG related $CH_4$ emissions between the western and eastern half. Assuming similar atmospheric mixing and dispersion conditions in the eastern half as in the western half, lower emissions would produce smaller enhancements, which matches observations.

Though $C_2H_6$ mixing ratios over the eastern half of the study area were generally lower than those observed over the western half, a raster flight on October 6 revealed $C_2H_6$ enhancements in the northeastern section of the study area (**Figure 8**). ERs on the four legs of this flight with $C_2H_6$ mixing ratios above 3.5 ppb (shown in light blue on **Figure 8**) were 1.5 ± 0.1%, 2.0 ± 0.1%, 2.5 ± 0.2%, and 7.1 ± 0.2%. The plume with an ER of 7.1% (shown in red on **Figure 8**) represents a localized enhancement in both $CH_4$ and $C_2H_6$.

### *3.3. Attribution of emissions*

The mean fraction of $CH_4$ emissions attributable to NG sources in the western half of the study area was calculated using Eq. 7. With $[C_2H_6/CH_4]_{area}$ = 1.21 ± 0.02% and $[C_2H_6/CH_4]_{NG}$ = 1.34 ± 0.03%, the mean estimate of the portion of the total $CH_4$ emissions originating from NG related sources in the western half of the study area was 90 ± 5% (1-sigma), and the portion of the total $CH_4$ emissions originating from other sources was estimated to be 10 ± 5%.

Our estimate for the portion of total $CH_4$ emissions originating from NG sources compares well with bottom-up estimates made for the western half of the study area by Vaughn et al. (2018). Bottom-up emission estimates were made for the two afternoons during which the mass balance flights used by Schwietzke et al. (2017) to calculate total $CH_4$ emissions occurred. Vaughn et al. (2018) estimated 89.9% and 87.8% of total $CH_4$ emissions in the western half to have originated from NG sources on October 1 and October 2, 2015, respectively, yielding a mean of 88.8%. The highest estimated $CH_4$ emissions from non-NG sources were from beef cattle and geologic seeps (Schwietzke et al., 2017).

Several factors prevented attribution of $CH_4$ emissions in the eastern half. First, $CH_4$ and $C_2H_6$ enhancements measured by the aircraft in the planetary boundary layer over the eastern half were low compared to those in the western half (as shown in **Figure 8** and by Schwietzke et al. (2017). In particular, the signal to noise ratio for the $C_2H_6$ enhancements onboard the aircraft was too low over the eastern half to allow estimation of ERs for aerial plumes mapped over the subregion. The $C_2H_6$ enhancements were

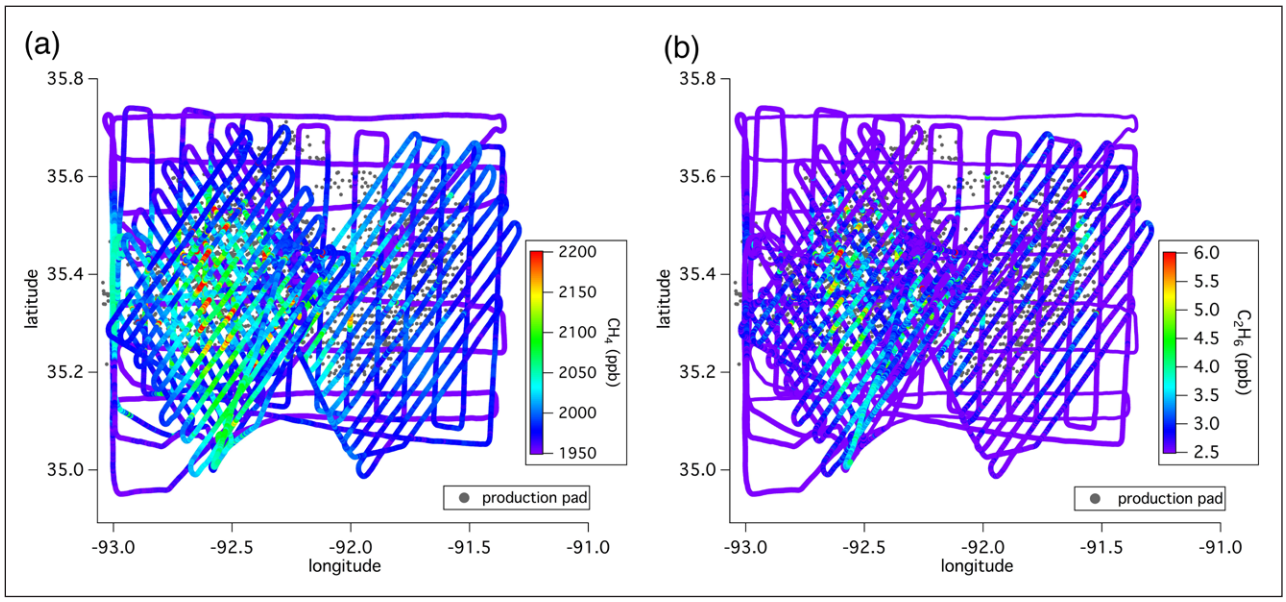


**Figure 8: $CH_4$ and $C_2H_6$ mole fractions on flights used for $CH_4$ attribution. (a)** Flight tracks from five raster flights on September 22 and October 2, 5, 6, and 7, 2015 color-coded by $CH_4$ mole fraction. **(b)** Flight tracks color-coded by $C_2H_6$ mole fraction. DOI: https://doi.org/10.1525/elementa.351.f8

also too low along the downwind transects of the two mass balance flights analyzed by Schwietzke et al. (2017) to determine a mass balance estimation of the $C_2H_6$ emissions for the entire study region, with $C_2H_6$ ranges on the downwind transects on October 1st and 2nd of 0.8 to 2.4 ppb and 1.0 to 2.0 ppb, respectively.

## 4. Conclusions

Ground-based, atmospheric measurements were used to determine a representative range of $C_2H_6$ to $CH_4$ facility-level plume ERs, confirmed by produced gas composition data. Using airborne and mobile surface atmospheric measurements of $C_2H_6$ and $CH_4$ and a simple two source mixing model, we show that 85–95% of total $CH_4$ emissions in the western half of the study area originate from NG operations. The western half represents 76% of total study area $CH_4$ emissions based on aircraft measurements (Schwietzke et al., 2017). Our result agrees with the NG $CH_4$ emissions estimate from a bottom-up model combining field measurements and spatiotemporal NG operations data by Vaughn et al. (2018).

Attribution of $CH_4$ emissions in the eastern half of the study area was not possible due to low boundary layer enhancements in $CH_4$ and $C_2H_6$. Low signal to noise for $C_2H_6$ also prohibited the use of the aircraft mass balance model for obtaining a $C_2H_6$ flux in both halves of the study area. Additionally, the assumption of a single mode NG ER distribution is not valid for the eastern half due to the more complex NG ER distribution.

The spatial variability in ER across the study area, as demonstrated by the difference in ER distributions in the western half compared with the eastern half, is important to account for when developing aggregated source emission signatures in a NG producing region. Although the majority of NG ERs observed in both the western and eastern halves fall in the same range of 1.2 to 1.5%, the eastern half has a second mode in its distribution, in which 34% of measured facilities have ERs of 2% or greater.

The Fayetteville Shale was chosen for the field campaign partly because $CH_4$ emissions from sources other than NG systems were expected to be low, making $CH_4$ source attribution less complicated than in areas with many potential $CH_4$ sources. Results from this study confirm that NG operations are the primary source of $CH_4$ in the western portion of the study area. Poultry farms were not found to be a significant source of $CH_4$.

Use of a ML facilitated the collection of an extensive amount of data on specific types of NG facilities and their $C_2H_6$ to $CH_4$ source signatures. For facility emission sampling, the ML was positioned directly adjacent to and downwind of the target facility such that ERs could be assigned to specific facilities. Fast response $C_2H_6$ and $CH_4$ in situ measurements made it possible to determine ERs in multiple plumes downwind of individual emission sources, yielding robust facility-level statistics compared to those from a simple linear regression using a small number of discrete flask samples collected in sources plumes or background conditions at different locations and times. Since ML routes were restricted only by public road access, it was possible to perform repeat measurements downwind of several facilities and examine day-to-day ER variability. With the exception of one production pad at which some combustion was likely occurring, ERs at all seven facilities with repeated measurements over several days were consistent over time (<10% variation), suggesting that measurements of $C_2H_6$ and $CH_4$ by ML surveys represent daily ERs at a given facility during the campaign.

Aircraft measurements in the atmospheric boundary layer were critical for obtaining information about area-integrated emission signals. By flying over and downwind of the entire western half of the study area, where $CH_4$ and $C_2H_6$ enhancements were greatest, the aircraft

sampled area plumes in the western half and provided a representative ER for the mix of emission sources.

The attribution model used in this study assumes that all $C_2H_6$ emissions originate from NG sources. Additionally, mean ERs for NG and total emissions are assumed to remain constant from day to day. The two-source model can only be applied in a simple case with two source categories with a single mode each, and would not be appropriate for use in an area with more complicated mix of sources and source signatures, including wetter gas and oil production, which could introduce other modes in the ER distribution. A complex mix of co-located sources with several different source signatures can present a challenge in that multiple tracers or constraints may be required for attribution. In such a case, a representative sample population of facility plumes with sufficient signal to noise may be used as a proxy for the mix of emissions as in Smith et al. (2015), preferably for multiple days and different flight paths. To further advance the value of top-down methods, it would be beneficial to test how stable the emission estimates and attribution solution are for different flight patterns, wind configurations, and dates/seasons, and to have access to composition data for key emission sources in a study region.

## Data Accessibility Statement

Enhancement ratios obtained by the mobile laboratories are uploaded in Microsoft Excel .xlsx format. NOAA mobile laboratory $C_2H_6$ and $CH_4$ enhancements relative to the local background are provided for ten different facilities (Sites 1–10) as text files. Files for the remaining 104 facilities can be provided upon request. Due to a governance agreement with project sponsors, locations of high frequency in situ ground measurements cannot be published. Aircraft data for the flights used for attribution and all discrete flask data are provided. Data are available at the following address: ftp://aftp.cmdl.noaa.gov/data/campaign/mls/RPSEA2015/.

## Supplemental files

The supplemental files for this article can be found as follows:

- **Section 1.** Mobile laboratory calibration protocol. DOI: https://doi.org/10.1525/elementa.351.s1
- **Section 2.** Description of mobile laboratory set-up. DOI: https://doi.org/10.1525/elementa.351.s1
- **Section 3.** Linearity and saturation of TILDAS instruments. DOI: https://doi.org/10.1525/elementa.351.s1
- **Section 4.** Flask measurements of $C_2H_6$ by gas chromatography mass spectrometry. DOI: https://doi.org/10.1525/elementa.351.s1
- **Section 5.** Flight patterns. DOI: https://doi.org/10.1525/elementa.351.s1
- **Section 6.** Determination of $C_2H_6$ to $CH_4$ enhancement ratios using mobile laboratory in situ data. DOI: https://doi.org/10.1525/elementa.351.s1
- **Section 7.** ERs for a production pad with evidence of combustion. DOI: https://doi.org/10.1525/elementa.351.s1
- **Section 8.** $C_2H_6$ to $CH_4$ ERs determined by aircraft spirals. DOI: https://doi.org/10.1525/elementa.351.s1
- **Section 9.** Poultry farm measurements. DOI: https://doi.org/10.1525/elementa.351.s1
- **Section 10.** Delaunay Triangulation Method. DOI: https://doi.org/10.1525/elementa.351.s1
- **Section 11.** Area-scale $C_2H_6$ to $CH_4$ ERs from each flight transect or leg. DOI: https://doi.org/10.1525/elementa.351.s1
- **Section 12.** Comparison of in situ $C_2H_6$ to $CH_4$ enhancement ratios with discrete flask samples. DOI: https://doi.org/10.1525/elementa.351.s1
- **Dataset S1.** Enhancement_ratios.xlsx. DOI: https://doi.org/10.1525/elementa.351.s2

## Acknowledgements

We thank members of our Technical Review Committee, F. George, G. Jersey, P. Lacey, T. Rufael, and D. Sundararajan, for their feedback and guidance during the data analysis and writing process. We also thank Southwestern Energy for providing a parking site with power for the mobile laboratory during the field campaign.

## Funding information

Funding for this work was provided by the Research Partnership to Secure Energy for America/National Energy Technology Laboratory contract no. 12122-95/DE-AC26-07NT42677 to the Colorado School of Mines, with additional equal contributions from the Colorado Energy Research Collaboratory, the National Oceanic and Atmospheric Administration, Southwestern Energy, XTO Energy (a subsidiary of ExxonMobil), Chevron, Statoil, and the American Gas Association.

## Competing interests

The authors have no competing interests to declare.

## Author contributions

- Substantial contributions to conception and design: IMM, GP, DZ, SS, SC, TV, CB, RS
- Acquisition of data: GP, ET, JK, PH, SCH, SC, SS, BM, BH, ED, PL, SW, EM, MC, AC, MR, DK
- Analysis and interpretation of data: GP, SS, TIY, DZ
- Drafting the article or revising it critically for important intellectual content: GP, SS, TIY, BM
- Final approval of the version to be published: All authors

## References

**Aircraft program methods.** 2018. Available at: https://www.esrl.noaa.gov/gmd/ccgg/aircraft/sampling.html. Accessed 2018 August 6.

**Alvarez, RA, Zavala-Araiza, D, Lyon, DR, Allen, DT, Barkley, ZR, Brandt, AR, Davis, KJ, Herndon, SC, Jacob, DJ, Karion, A, Kort, EA, Lamb, BK, Lauvaux, T, Maasakkers, JD, Marchese, AJ, Omara, M, Pacala, SW, Peischl, J, Robinson, AL, Shepson, PB, Sweeney, C, Townsend-Small, A, Wofsy, SC** and **Hamburg, SP.** 2018. Assessment of methane emissions from the U.S. oil and gas supply chain. *Science* **361**(1693): 1–8. DOI: https://doi.org/10.1126/science.aar7204

**Arkansas Geological Survey.** 2015. Natural gas. Available at: https://www.geology.arkansas.gov/energy/natural-gas-in-arkansas.html. Accessed 2018 August 6.

**Arkansas Oil and Gas Commission (AOGC).** 2015. Fayetteville shale gas sales. Available at: http://www.aogc.state.ar.us/sales/shale.aspx. Accessed 2018 August 6.

**Bell, CS, Vaughn, TL, Zimmerle, DJ, Herndon, SC, Yacovitch, TI, Heath, GA, Pétron, G, Edie, R, Field, RA, Murphy, SM, Robertson, AM** and **Soltis, J.** 2017. Comparison of methane emission estimates from multiple measurement techniques at natural gas production pads. *Elem Sci Anth* **5**: 79. DOI: https://doi.org/10.1525/elementa.266

**Brandt, AR, Heath, GA, Kort, EA, O'Sullivan, F, Pétron, G, Jordaan, SM, Tans, P, Wilcox, J, Gopstein, AM, Arent, D, Wofsy, S, Brown, NJ, Bradley, R, Stucky, GD, Eardley, D** and **Harriss, R.** 2014. Methane leaks from North American natural gas systems. *Science* **343**(6172): 733–735. DOI: https://doi.org/10.1126/science.1247045

**Caulton, DR, Shepson, PB, Santoro, RL, Sparks, JP, Howarth, RW, Ingraffea, AR, Cambaliza, MOL, Sweeney, C, Karion, A, Davis, KJ, Stirm, BH, Montzka, SA** and **Miller, BR.** 2014. Toward a better understanding and quantification of methane emissions from shale gas development. *P Natl Acad Sci USA* **111**(17): 6237–6242. DOI: https://doi.org/10.1073/pnas.1316546111

**Conley, S, Faloona, I, Mehrotra, S, Suard, M, Lenschow, DH, Sweeney, C, Herndon, SC, Schwietzke, S, Pétron, G, Pifer, J, Kort, EA** and **Schnell, R.** 2017. Application of Gauss's Theorem to quantify localized surface emissions from airborne measurements of wind and trace gases. *Atmos Meas Tech* **10**: 3345–3358. DOI: https://doi.org/10.5194/amt-10-3345-2017

**Dlugokencky, EJ, Steele, LP, Lang, PM** and **Masarie, KA.** 1994. The growth rate and distribution of atmospheric methane. *J Geophys Res Atmos* **99**: 17021–17043. DOI: https://doi.org/10.1029/94JD01245

**Earth System Research Laboratory (ESRL).** 2017. Global greenhouse gas reference network. Available at: http://www.esrl.noaa.gov/gmd/ccgg. Accessed 2018 August 6.

**EIA.** 2016. Carbon dioxide emissions coefficients. Available at: https://www.eia.gov/environment/emissions/co2_vol_mass.php Accessed 2018 August 6.

**EIA.** 2017. U.S. dry natural gas production. Available at: https://www.eia.gov/dnav/ng/hist/n9070us2A.htm. Accessed 2018 August 6.

**EPA.** 2017. Inventory of U.S. greenhouse gas emissions and sinks: 1990–2015. Available at: https://www.epa.gov/sites/production/files/2017-02/documents/2017_complete_report.pdf. Accessed 2018 August 6.

**Frankenberg, C, Thorpe, AK, Thompson, DR, Hulley, G, Kort, EA, Vance, N, Borchardt, J, Krings, T, Gerilowski, K, Sweeney, C, Conley, S, Bue, BD, Aubrey, AD, Hook, S** and **Green, RO.** 2016. Airborne methane remote measurements reveal heavy-tail flux distribution in Four Corners region. *P Natl Acad Sci USA* **35**(35): 9734–9739. DOI: https://doi.org/10.1073/pnas.1605617113

**Hopkins, FM, Kort, EA, Bush, SE, Ehleringer, JR, Lai, C-T, Blake, DR** and **Randerson, JT.** 2016. Spatial patterns and source attribution of urban methane in the Los Angeles Basin. *J Geophys Res-Atmos* **121**(5): 2490–2507. DOI: https://doi.org/10.1002/2015JD024429

**Karion, A, Sweeney, C, Kort, EA, Shepson, PB, Brewer, A, Cambaliza, M, Conley, S, Davis, K, Deng, A Hardesty, M, Herndon, SC, Lauvaux, T, Lavoie, T, Lyon, D, Newberger, T, Pétron, G, Rella, C, Smith, M, Wolter, S, Yacovitch, TI** and **Tans, P.** 2015. Aircraft-based estimate of total methane emissions from the Barnett Shale region. *Environ Sci Technol* **49**(13): 8124–8131. DOI: https://doi.org/10.1021/acs.est.5b00217

**Karion, A, Sweeney, C, Pétron, G, Frost, G, Hardesty, RM, Kofler, J, Miller, BR, Newberger, T, Wolter, S, Banta, R, Brewer, A, Dlugokencky, E, Lang, PM, Montzka, SA, Schnell, R, Tans, P, Trainer, M, Zamora, R** and **Conley, S.** 2013. Methane emissions estimate from airborne measurements over a western United States natural gas field. *Geophys Res Lett* **40**(16): 4393–4397. DOI: https://doi.org/10.1002/grl.50811

**Kort, EA, Smith, ML, Murray, LT, Gvakharia, A, Brandt, AR, Peischl, J, Ryerson, TB, Sweeney, C** and **Travis, K.** 2016. Fugitive emissions from the Bakken shale illustrate role of shale production in global ethane shift. *Geophys Res Lett* **43**(9): 4617–4623. DOI: https://doi.org/10.1002/2016GL068703

**Monteny, GJ, Groenestein, CM** and **Hilhorst, MA.** 2001. Interactions and coupling between emissions of methane and nitrous oxide from animal husbandry. *Nutr Cycl Agroecosys* **60**: 123–132. DOI: https://doi.org/10.1023/A:1012602911339

**Nisbet, EG, Dlugokencky, EJ, Manning, MR, Lowry, D, Fisher, RE, France, JL, Michel, SE, Miller, JB, White, JWC, Vaughn, B, Bousquet, P, Pyle, JA, Warwick, NJ, Cain, M, Brownlow, R, Zazzeri, G, Lanoisellé, M, Manning, AC, Gloor, E, Worthy, DEJ, Brunke, E-G, Labuschagne, C, Wolff, EW** and **Ganesan, AL.** 2016. Rising atmospheric methane: 2007–2014 growth and isotopic shift. *Global Biogeochem Cy* **30**(9): 1356–1370. DOI: https://doi.org/10.1002/2016GB005406

**Ogejo, JA** and **Collins, ER, Jr.** 2009. Storing and handling poultry litter. Virginia Polytechnic Institute and State Unversity, Virginia Cooperative Extension. 422–054. Available at: https://pubs.ext.vt.edu/content/dam/pubs_ext_vt_edu/442/442-054/442-054_pdf.pdf. Accessed 2018 December 21.

**Peischl, J, Karion, A, Sweeney, C, Kort, EA, Smith, ML, Brandt, AR, Yeskoo, T, Aikin, KC, Conley, S, Gvakharia, A, Trainer, M, Wolter, S** and **Ryerson, TB.** 2016. Quantifying atmospheric methane emissions from oil and natural gas production in the

Bakken shale region of North Dakota. *J Geophys Res Atmos* **121**(10): 6101–6111. DOI: https://doi.org/10.1002/2015JD024631

**Peischl, J, Ryerson, TB, Aikin, KC, de, Gouw, JA, Gilman, JB, Holloway, JS, Lerner, BM, Nadkarni, R, Neuman, JA, Nowak, JB, Trainer, M, Warneke, C** and **Parrish, DD.** 2015. Quantifying atmospheric methane emissions from the Haynesville, Fayetteville, and northeastern Marcellus shale gas production regions. *J Geophys Res Atmos* **120**(5): 2119–2139. DOI: https://doi.org/10.1002/2014JD022697

**Pétron, G, Frost, G, Miller, BR, Hirsch, AI, Montzka, SA, Karion, A, Trainer, M, Sweeney, C, Andrews, AE, Miller, L, Kofler, J, Bar-Ilan, A, Dlugokencky, E, Patrick, L, Moore, CT, Jr., Ryerson, TB, Siso, C, Kolodzey, W, Lang, PM, Conway, T, Novelli, P, Masarie, K, Hall, B, Guenther, D, Kitzis, D, Miller, J, Welsh, D, Wolf, D, Neff, W** and **Tans, P.** 2012. Hydrocarbon emissions characterization in the Colorado Front Range: A pilot study. *J Geophys Res* **117**(D4): D404304. DOI: https://doi.org/10.1029/2011JD016360

**Pétron, G, Karion, A, Sweeney, C, Miller, BR, Montzka, SA, Frost, G, Trainer, M, Tans, P, Andrews, AE, Kofler, J, Helmig, D, Guenther, D, Dlugokencky, E, Lang, PM, Newberger, T, Wolter, S, Hall, B, Novelli, P, Brewer, A, Conley, S, Hardesty, M, Banta, R, White, A, Noone, D, Wolfe, D** and **Schnell, R.** 2014. A new look at methane and nonmethane hydrocarbon emissions from oil and natural gas operations in the Colorado Denver-Julesburg Basin. *J Geophys Res Atmos* **119**(11): 6836–6852. DOI: https://doi.org/10.1002/2013JD021272

**Robertson, AM, Edie, R, Snare, D, Soltis, J, Field, RA, Burkhart, MD, Bell, CS, Zimmerle, DJ** and **Murphy, SM.** 2017. Variation in methane emission rates from well pads in four oil and gas basins with contrasting production volumes and compositions. *Environ Sci Technol* **51**(15): 8832–8840. DOI: https://doi.org/10.1021/acs.est.7b00571

**Roscioli, JR, Yacovitch, TI, Floerchinger, C, Mitchell, AL, Tkacik, DS, Subramanian, R, Martinez, DM, Vaughn, TL, Williams, L, Zimmerle, DJ, Robinson, AL, Herndon, SC** and **Marchese, AJ.** 2015. Measurements of methane emissions from natural gas gathering facilities and processing plants: Measurement methods. *Atmos Meas Tech* **8**(5): 2017–2035. DOI: https://doi.org/10.5194/amt-8-2017-2015

**Rudolph, J** and **Enhalt, DH.** 1981. Measurements of $C_2$-$C_5$ hydrocarbons over the North Atlantic. *J Geophys Res* **86**(C12): 11959–11964. DOI: https://doi.org/10.1029/JC086iC12p11959

**Schwietzke, S, Pétron, G, Conley, S, Pickering, C, Mielke-Maday, I, Dlugokencky, E, Tans, P, Vaughn, TL, Bell, CS, Zimmerle, DJ, Wolter, S, King, CW, White, AB, Coleman, T, Biano, L** and **Schnell, R.** 2017. Improved mechanistic understanding of natural gas methane emissions from spatially resolved aircraft measurements. *Environ Sci Technol* **51**(12): 7286–7294. DOI: https://doi.org/10.1021/acs.est.7b01810

**Smith, ML, Gvakharia, A, Kort, EA, Sweeney, C, Conley, S, Faloona, I, Newberger, T, Schnell, R, Schwietzke, S** and **Wolter, S.** 2017. Airborne quantification of methane emissions over the Four Corners region. *Environ Sci Technol* **51**(10): 5832–5837. DOI: https://doi.org/10.1021/acs.est.6b06107

**Smith, ML, Kort, EA, Karion, A, Sweeney, C, Herndon, SC** and **Yacovitch, TI.** 2015. Airborne ethane observations in the Barnett Shale: Quantification of ethane flux and attribution of methane emissions. *Environ Sci Technol* **49**(13): 8158–8166. DOI: https://doi.org/10.1021/acs.est.5b00219

**Townsend-Small, A, Marrero, JE, Lyon, DR, Simpson, IJ, Meinardi, S** and **Blake, DR.** 2015. Integrating source apportionment tracers into a bottom-up inventory of methane emissions in the Barnett Shale hydraulic fracturing region. *Environ Sci Technol* **49**(13): 8175–8182. DOI: https://doi.org/10.1021/acs.est.5b00057

**USDA.** 2015. State-level poultry production data. Available at: https://quickstats.nass.usda.gov/results/B2269209-0E29-3655-B48E-F8BCDDB62A65. Accessed 2018 August 6.

**Vaughn, TL, Bell, CS, Pickering, CK, Schwietzke, S, Heath, G, Pétron, G, Zimmerle, DJ, Schnell, RC** and **Nummedal, D.** 2018. Temporal variability largely explains top-down/bottom-up difference in methane emissions estimates from a natural gas production region. *P Natl Acad Sci USA* **115**(46): 11712–11717. DOI: https://doi.org/10.1073/pnas.1805687115

**Vaughn, TL, Bell, CS, Yacovitch, TI, Roscioli, JR, Herndon, SC, Conley, S, Schwietzke, S, Health, GA, Pétron, G** and **Zimmerle, DJ.** 2017. Comparing facility-level methane emission rate estimates at natural gas gathering and boosting stations. *Elem Sci Anth*, **5**: 71. DOI: https://doi.org/10.1525/elementa.257

**Visschedijk, AJH, Denier van der Gon, HAC, Doornenbal, HC** and **Cremonese, L.** 2018. Methane and ethane emission scenarios for potential shale gas production in Europe. *Adv Geosci* **45**: 125–131. DOI: https://doi.org/10.5194/adgeo-45-125-2018

**Yacovitch, TI, Daube, C, Vaughn, TL, Bell, CS, Roscioli, JR, Knighton, WB, Nelson, DD, Zimmerle, DJ, Pétron, G** and **Herndon, SC.** 2017. Natural gas facility methane emissions: Measurements by tracer flux ratio in two US natural gas producing basins. *Elem Sci Anth* **5**: 69. DOI: https://doi.org/10.1525/elementa.251

**Yacovitch, TI, Herndon, SC, Pétron, G, Kofler, J, Lyon, D, Zahniser, MS** and **Kolb, CE.** 2015. Mobile laboratory observations of methane emissions in the Barnett Shale region. *Environ Sci Technol* **49**(13): 7889–7895. DOI: https://doi.org/10.1021/es506352j

**Yacovitch, TI, Herndon, SC, Roscioli, JR, Floerchinger, C, McGovern, RM, Agnese, M, Pétron, G, Kofler, J, Sweeney, C, Karion, A, Conley, S, Kort, EA, Nähle,**

**L, Fischer, M, Hildebrandt, L, Koeth, J, McManus, JB, Nelson, DD, Zahniser, MS** and **Kolb, CE.** 2014. Demonstration of an ethane spectrometer for methane source identification. *Environ Sci Technol* **48**(14): 8028–8034. DOI: https://doi.org/10.1021/es501475q

**Zavala-Araiza, D, Lyon, DR, Alvarez, RA, Davis, KJ, Harriss, R, Herndon, SC, Karion, A, Kort, EA, Lamb, BK, Lan, X, Marchese, AJ, Pacala, SW, Robinson, AL, Shepson, PB, Sweeney, C, Talbot, R, Townsend-Small, A, Yacovitch, TI, Zimmerle, DJ** and **Hamburg, SP.** 2015. Reconciling divergent estimates of oil and gas methane emissions. *P Natl Acad Sci USA* **112**(51): 15597–15602. DOI: https://doi.org/10.1073/pnas.1522126112

**Zimmerle, DJ, Pickering, CK, Bell, CS, Heath, GA, Nummedal, D, Pétron, P** and **Vaughn, TL.** 2017. Gathering pipeline methane emissions in Fayetteville shale pipelines and scoping guidelines for future pipeline measurement campaigns. *Elem Sci Anth* **5**: 70. DOI: https://doi.org/10.1525/elementa.258

**How to cite this article:** Mielke-Maday, I, Schwietzke, S, Yacovitch, TI, Miller, B, Conley, S, Kofler, J, Handley, P, Thorley, E, Herndon, SC, Hall, B, Dlugokencky, E, Lang, P, Wolter, S, Moglia, E, Crotwell, M, Crotwell, A, Rhodes, M, Kitzis, D, Vaughn, T, Bell, C, Zimmerle, D, Schnell, R and Pétron, G. 2019. Methane source attribution in a U.S. dry gas basin using spatial patterns of ground and airborne ethane and methane measurements. *Elem Sci Anth*, 7: 13. DOI: https://doi.org/10.1525/elementa.351

**Domain Editor-in-Chief:** Detlev Helmig, Institute of Alpine and Arctic Research, University of Colorado Boulder, US

**Associate Editor:** Brian Lamb, Washington State University, US

**Knowledge Domain:** Atmospheric Science

**Part of an *Elementa* Forum:** Oil and Natural Gas Development: Air Quality, Climate Science, and Policy

**Submitted:** 03 August 2018 **Accepted:** 26 February 2019 **Published:** 05 April 2019